REPORT DOCUMENTATION PAGE

Form Approved OMB NO. 0704-0188

1. AGENCY USE ONLY (Leave Blank)	2. REPORT DATE:	3. REPORT TYPE AND DATES COVERED
		New Reprint 7-Sep-2005 - 20-Oct-2005

4. TITLE AND SUBTITLE

Transport Properties of Sulfonated Poly(styrene-b-isobutylene-b-styrene) Triblock Copolymers at High Ion-Exchange Capacities

5. FUNDING NUMBERS

DAAD190310130

6. AUTHORS

Karen I. Winey, Yossef A. Elabd, Eugene Napadensky, Charles W. Walker

8. PERFORMING ORGANIZATION REPORT NUMBER

7. PERFORMING ORGANIZATION NAMES AND ADDRESSES

University of Pennsylvania
3451 Walnut Street
Room P221
Philadelphia, PA 19104 -

9. SPONSORING/MONITORING AGENCY NAME(S) AND ADDRESS(ES)

U.S. Army Research Office
P.O. Box 12211
Research Triangle Park, NC 27709-2211

10. SPONSORING / MONITORING AGENCY REPORT NUMBER

44990-CH.3

11. SUPPLEMENTARY NOTES

The views, opinions and/or findings contained in this report are those of the author(s) and should not contrued as an official Department of the Army position, policy or decision, unless so designated by other documentation.

12. DISTRIBUTION AVAILIBILITY STATEMENT

Approved for Public Release; Distribution Unlimited

12b. DISTRIBUTION CODE

13. ABSTRACT (Maximum 200 words)

The abstract is below since many authors do not follow the 200 word limit

14. SUBJECT TERMS

proton conductivity, SAXS, transport, morphology, block copolymer

15. NUMBER OF PAGES

Unknown due to possible attachments

16. PRICE CODE

17. SECURITY CLASSIFICATION OF REPORT	18. SECURITY CLASSIFICATION ON THIS PAGE	19. SECURITY CLASSIFICATION OF ABSTRACT	20. LIMITATION OF ABSTRACT
UNCLASSIFIED	UNCLASSIFIED	UNCLASSIFIED	UL

NSN 7540-01-280-5500

Standard Form 298 (Rev .2-89)
Prescribed by ANSI Std.
239-18 298-102

Report Title

Transport Properties of Sulfonated Poly(styrene-b-isobutylene-b-styrene) Triblock Copolymers at High Ion-Exchange Capacities

ABSTRACT

Transport properties of sulfonated poly(styrene-b-isobutylene-b-styrene) (S-SIBS) triblock copolymers were examined as a function of ion-exchange capacity (IEC), specifically at high IECs (up to ~2 mequiv/g). The proton conductivity of S-SIBS was ~1 order of magnitude higher than sulfonated polystyrene at similar IECs and 3-fold higher than Nafion 117 at an IEC of 2 mequiv/g. However, all polymers in this study possessed similar selectivities (i.e., proton conductivity/methanol permeability) regardless of chemistry or morphology. Smallangle X-ray scattering reveals a periodic-to-nonperiodic transition in S-SIBS with an anisotropic lamellar morphology oriented in the plane of the membrane at IECs ranging from 0.5 to 1 mequiv/g and an isotropic
cocontinuous morphology at IECs ranging from 1.1 to 2 mequiv/g. This morphological transition coincides with a discontinuity in the IEC-dependent transport properties. In addition, S-SIBS transport properties were measured
after solution casting from 15 different solvents at a constant IEC (0.8 mequiv/g). Transport properties varied by almost 3 orders of magnitude when comparing S-SIBS solution cast from toluene to a toluene/ethanol mixture.
X-ray scattering results show morphological differences with solvent choice. This study demonstrates the significant impact of morphology on transport properties in ionic block copolymers.

Transport Properties of Sulfonated Poly(styrene-*b*-isobutylene-*b*-styrene) Triblock Copolymers at High Ion-Exchange Capacities

Yossef A. Elabd,*,† Eugene Napadensky,‡ Charles W. Walker,§ and Karen I. Winey⊥

Department of Chemical and Biological Engineering, Drexel University, Philadelphia, Pennsylvania 19104; Weapons and Materials Research Directorate, U.S. Army Research Laboratory, Aberdeen Proving Ground, Maryland 21005; Sensors and Electron Devices Directorate, U.S. Army Research Laboratory, Adelphi, Maryland 20783; and Department of Materials Science and Engineering, University of Pennsylvania, Philadelphia, Pennsylvania 19104

Received September 7, 2005; Revised Manuscript Received October 20, 2005

ABSTRACT: Transport properties of sulfonated poly(styrene-*b*-isobutylene-*b*-styrene) (S-SIBS) triblock copolymers were examined as a function of ion-exchange capacity (IEC), specifically at high IECs (up to ∼2 mequiv/g). The proton conductivity of S-SIBS was ∼1 order of magnitude higher than sulfonated polystyrene at similar IECs and 3-fold higher than Nafion 117 at an IEC of 2 mequiv/g. However, all polymers in this study possessed similar selectivities (i.e., proton conductivity/methanol permeability) regardless of chemistry or morphology. Small-angle X-ray scattering reveals a periodic-to-nonperiodic transition in S-SIBS with an anisotropic lamellar morphology oriented in the plane of the membrane at IECs ranging from 0.5 to 1 mequiv/g and an isotropic cocontinuous morphology at IECs ranging from 1.1 to 2 mequiv/g. This morphological transition coincides with a discontinuity in the IEC-dependent transport properties. In addition, S-SIBS transport properties were measured after solution casting from 15 different solvents at a constant IEC (0.8 mequiv/g). Transport properties varied by almost 3 orders of magnitude when comparing S-SIBS solution cast from toluene to a toluene/ethanol mixture. X-ray scattering results show morphological differences with solvent choice. This study demonstrates the significant impact of morphology on transport properties in ionic block copolymers.

1. Introduction

Ion conducting polymers containing strong acidic groups (e.g., sulfonic acid) are of interest for a variety of applications, such as sensors, actuators, ion-exchange membranes, and fuel cells. Fuel cells in particular have received tremendous attention because of their potential to achieve higher efficiencies than current power sources with renewable fuels at a lower environmental cost.[1] In the fuel cell, the ion conducting polymer or proton exchange membrane (PEM) serves as both a cell separator, separating the anode from the cathode, and an electrolyte, conducting protons from the anode to the cathode. Despite the numerous advantages of fuel cells, there are several key problems with PEMs that hinder fuel cell efficiency, such as low proton conductivity at higher temperatures, poor water management, and high fuel crossover. Fuel crossover is a main concern as it applies to the methanol fuel-based PEM fuel cell (also known as the direct methanol fuel cell (DMFC)). Methanol diffusion (methanol crossover) across the PEM hinders fuel cell efficiency, by a loss in fuel, cathode voltage, and overall fuel cell lifetime.[2]

The most frequently used PEM in fuel cells, Nafion (DuPont), a perfluorosulfonic acid polymer, exhibits sufficient proton conductivity at optimal water contents and is thermally, chemically, and oxidatively stable. However, Nafion suffers from low conductivity at high temperatures and high methanol crossover. Current research is focused on developing Nafion replacements that are durable, lower in cost, higher in proton conductivity at higher temperatures, maintain an adequate water balance, and are resistant to methanol.[3]

Early investigations on PEMs revealed that transport properties are dependent on polymer morphology or ionic nanostructure.[4,5] There are a number of publications that examine the structure of PEMs, particularly Nafion, using a variety of techniques. The details of these findings have recently been reviewed by Mauritz and Moore.[6] Although there are diverse opinions regarding the detailed morphology, there is a consensus that microphase separation occurs in PEMs. Aggregates of ions form due to the electrostatic interactions between ion pairs, leading to the formation of two microphases: ion-rich and ion-poor domains. Ion-rich domains are referred to as ionic aggregates, while ion-poor domains are mostly the hydrophobic part or backbone of the polymer. Increasing ion or sulfonic acid content in the polymer transforms the polymer from an insulator to an ion conductor (percolation threshold), whereby isolated ionic domains become interconnected throughout the polymer. Above this percolation threshold, protons transport across the PEM via hydrolyzed acidic sites through this interconnected ionic network. A number of investigations have demonstrated that increasing ion content in PEMs results in an increase in proton transport, water uptake, and methanol crossover.[7−10] Also, it is evident that the diffusion of protons, water, and methanol is affected by the ionic nanostructure and follows a percolation model.[10−15]

More specifically, several recent investigations have clearly demonstrated the effects of ordered and oriented ionic nanostructures on transport properties. Ding et al.[16] demonstrated increased proton conductivity in polystyrene grafted with poly(styrenesulfonic acid) side chains compared to a random

† Drexel University.
‡ Weapons and Materials Research Directorate, U.S. Army Research Laboratory.
§ Sensors and Electron Devices Directorate, U.S. Army Research Laboratory.
⊥ University of Pennsylvania.
* To whom correspondence should be addressed: Ph 215-895-0986; Fax 215-895-5837; e-mail elabd@drexel.edu.

10.1021/ma051958n CCC: $33.50
Published on Web 12/01/2005

copolymer of polystyrene and poly(styrenesulfonic acid) (i.e., sulfonated polystyrene). They concluded that the increase in proton conductivity was attributed to a more ordered ionic nanostructure. Cable et al.[17] stretched Nafion to induce orientation of ionic nanostructure and demonstrated a 40% difference in conductivity when comparing measurements parallel and perpendicular to the plane of the membrane (anisotropic conductivity). Maki-Ontto et al.[18] also demonstrated anisotropic conductivity (an order of magnitude difference) in proton conductive block copolymers that were sheared to induce an oriented lamellar nanostructure. Similarly, in our laboratory, anisotropic conductivity was observed when comparing measurements parallel and perpendicular to the plane of the membrane for sulfonated poly(styrene-*b*-isobutylene-*b*-styrene) block copolymers that possess a lamellar morphology oriented in the plane of the membrane.[19]

Ion conducting block copolymers in which only one of the blocks is sulfonated or ionic are attractive because they conjoin the concepts of two different materials (block copolymers and PEMs). Block copolymers provide a unique template, where microphase separation occurs on a nanometer scale due to the thermodynamic incompatibility between unlike blocks forming a variety of self-assembled morphologies including spheres arranged on a cubic lattice, hexagonally packed cylinders, interpenetrating gyroids, and alternating lamellae.[20] For ion conducting block copolymers, only one of the microdomains contains the ionic nanostructure (~1 nm), while the block copolymer morphology is on the order of 10 nm. A study by Wiess et al.,[21] using X-ray scattering on sulfonated poly(styrene-*b*-(ethylene-*r*-butylene)-*b*-styrene), confirms these coexisting length scales with 3−4 nm for the ionic domains and 20−30 nm for the block copolymer morphology. Sulfonated block copolymers are intriguing materials because the combination of different block (ionic and nonionic) properties provides the potential for unique ordered ionic morphologies, where transport properties can be tailored.

Initial studies on sulfonated block copolymers focused only on the sulfonation and the structural and thermal characterization of styrene-based block copolymers at low ion-exchange capacities (IECs).[21−26] These reports did not address transport properties. Recently, a number of investigators have examined the transport properties of sulfonated block copolymers at higher IECs (~1−2 mequiv/g) and have shown comparable conductivities to Nafion (0.91 mequiv/g).[29−32] Several studies report nonperiodic morphologies at higher IECs; however, it is still unclear how the block copolymer structure is affected as a function of IEC (particularly at higher IECs) and its subsequent effect on transport properties.[31,32] In this study, structure−transport property relationships are examined for sulfonated poly(styrene-*b*-isobutylene-*b*-styrene) block copolymers as a function of IEC (up to ~2 mequiv/g). Additionally, the effects of casting solvent choice and annealing temperature on the ionic block copolymer morphology are investigated.

2. Experimental Section

2.1. Materials. Poly(styrene-*b*-isobutylene-*b*-styrene) (SIBS) triblock copolymer (TS-3000S, lot. no. 990215) was provided by Kuraray Co., Ltd., Tsukuba Research Laboratories with these reported properties: 19.36 mol % (30.84 wt %) styrene, 0.95 specific gravity, M_w = 71 920 g/mol, M_n = 48 850 g/mol, and PDI = 1.47. Polystyrene (PS) was purchased from Scientific Polymer Products, Inc., with the reported properties: M_w = 260K g/mol, 1.05 specific gravity, and T_g = 100 °C. SIBS and PS were both used as received. Nafion 117 was obtained from C.G. Processing, Inc. (1100 equiv weight). The Nafion membranes were pretreated, and the details of this procedure are reported elsewhere.[10] Other chemicals used in this study are as follows: toluene (EM Science, assay 99.5%), hexanol (J.T. Baker, 99%), methylene chloride (EM Science, HPLC grade), methanol (EM Scientific, HPLC grade), tetrahydrofuran (THF) (Burdick & Jackson, HPLC Grade), chloroform (Burdick & Jackson, HPLC grade), benzene (EM Science, HPLC Grade), cyclohexanol (EM Scientific, assay 98%), ethanol (Warner-Graham Co., 200 proof, anhydrous), 2-propanol (Burdick & Jackson, HPLC Grade), cyclohexanone (Aldrich, reagent grade), butanol (J.T. Baker, reagent grade), and water (J.T. Baker, HPLC grade).

Table 1. Polymer Membranes (Nafion 117, Sulfonated Polystyrene (S-PS), Sulfonated Poly(styrene-*b*-isobutylene-*b*-styrene (S-SIBS)) as a Function of Ion Content

sample name	sulfonation level (mol %)	IEC (mequiv/g)	sample name	sulfonation level (mol %)	IEC (mequiv/g)
Nafion 117	NA	0.91	S-SIBS-25	25.26	0.71
S-PS-0[a]	0	0	S-SIBS-29	29.23	0.81
S-PS-6[a]	5.68	0.52	S-SIBS-34	34.33	0.94
S-PS-14	14.18	1.23	S-SIBS-36	35.63	0.97
S-PS-15	15.13	1.30	S-SIBS-42	41.95	1.13
S-PS-24	23.70	1.92	S-SIBS-48	48.16	1.28
S-SIBS-0[a]	0	0	S-SIBS-54	53.68	1.41
S-SIBS-13[a]	12.50	0.36	S-SIBS-70	70.14	1.78
S-SIBS-13	12.50	0.36	S-SIBS-79	79.05	1.97
S-SIBS-17	16.60	0.47	S-SIBS-82	82.41	2.04
S-SIBS-22	22.49	0.63			

[a] Solution cast from toluene. All other samples were solvent cast from a 85/15 (w/w) mixture of toluene/hexanol, with the exception of Nafion 117.

2.2. Membrane Preparation. The styrene monomeric units in SIBS were sulfonated in solution with methylene chloride as the solvent and acetyl sulfate as the sulfonating agent. The details of this sulfonation protocol are described elsewhere.[10,33] PS was sulfonated in this study with the same procedure used for sulfonating SIBS. The ion-exchange capacity (IEC) (or mol % sulfonation) of each polymer in this study was determined by elemental analysis (EA), and the results are listed in Table 1. Hereafter, sulfonated SIBS and PS are referred to as S-SIBS-# and S-PS-#, respectively, where S-SIBS represents sulfonated poly(styrene-*b*-isobutylene-*b*-styrene) and S-PS represents sulfonated polystyrene. The succeeding number, #, refers to the mol % sulfonation, which is defined as

$$\text{mol \%} = \left(\frac{\text{moles of sulfonic acid}}{\text{moles of styrene}}\right) \times 100 \qquad (1)$$

and the IEC is defined as the milliequivalents of sulfonic acid per gram of polymer (mequiv/g).

After sulfonation and purification of each polymer, S-SIBS and S-PS, ranging from 13 to 82 mol % and 14 to 24 mol % sulfonation, respectively, were dissolved in a mixed solvent of toluene/hexanol (85/15, w/w) at concentrations ranging from 2.5 to 5% (w/v). Polymer solutions were cast in open Teflon Petri dishes for ~1 week at ambient conditions. Solution-cast membranes were then annealed in a vacuum oven at 50 °C for an additional 2 weeks. S-SIBS-0, -13 and S-PS-0, -6 were cast similarly, but with pure toluene as the casting solvent. Note that S-SIBS-13 was solution cast from both toluene/hexanol (85/15, w/w) and toluene.

In addition to varying ion content, the effect of casting solvent choice on the polymer membrane at a constant ion content was also explored. S-SIBS-29 was solution cast from a number of different solvents: chloroform, methylene chloride, THF, cyclohexanol, benzene, cyclohexanone, toluene, and mixtures of toluene with ethanol, 2-propanol, butanol, and hexanol. Membranes solution cast from different solvents were all prepared similarly. Each polymer sample was dissolved in its respective solvent at concentrations ranging from 5 to 10% (w/v) and subsequently cast in open Teflon Petri dishes for ~3 weeks at ambient conditions. Solution-cast membranes were then placed under vacuum at room temperature for 24 h followed by annealing under vacuum at 80 °C for

48 h. S-SIBS-29 was solution-cast from cyclohexanone and cylohexanol with slightly different procedures. For cyclohexanone, a 6% (w/v) S-SIBS-29 solution was cast at ambient conditions for 3 weeks. The sample was then annealed at 60 °C for ∼7 weeks. For cyclohexanol, a 4% (w/v) S-SIBS-29 solution was cast by first annealing at 60 °C for 3 weeks. This procedure was followed by placing membranes under vacuum at room temperature for 24 h and then annealing under vacuum at 80 °C for another 48 h.

The effect of annealing temperature was also investigated. S-SIBS-0 and S-SIBS-22 were solution cast from toluene (5% (w/v)) in Teflon Petri dishes for ∼2 weeks at ambient conditions. Solution-cast membranes were then placed under vacuum at room temperature for an additional 2 weeks to remove any residual solvent. After this step, polymers were annealed under vacuum at either 50 or 170 °C for 1 day. S-SIBS-22 was also solution-cast from THF using the same procedure.

2.3. Conductivity. Proton conductivity of each membrane was measured using ac impedance spectroscopy. Measurements were collected between 10 Hz and 100 kHz using a Solartron ac impedance system (1260 impedance analyzer, 1287 electrochemical interface, Zplot software). Conductivity was measured perpendicular to the plane of the membrane with a two-electrode cell comprised of two 1.26 cm^2 stainless steel blocking electrodes. All membranes were prehydrated in deionized water for at least 24 h and then enclosed in a sealable cell to maintain hydration during impedance measurements. Conductivity was calculated from the real impedance, which was determined from the *x*-intercept of a linear fit of the imaginary vs real impedance data over a high-frequency range.[19] Conductivity values for each membrane reported in this study are an average of multiple (at least three) experiments, where the standard deviation was 5−10% of those values.

2.4. Permeability. The methanol permeability of each membrane was measured using a temperature-regulated side-by-side glass diffusion cell (PermeGear Inc.) with a real-time in-line Fourier transform infrared, attenuated total reflectance (FTIR-ATR) spectrometer for detection. The FTIR spectrometer (Nicolet Magna 560 series) was equipped with a temperature-controlled flow-through horizontal ATR cell (Specac Inc.). A multibounce zinc selenide ATR crystal (Specac Inc.) with a refractive index of 2.4 was used. Infrared spectra were continuously recorded throughout each experiment at 67 s intervals using 128 scans and 4 cm^{-1} resolution for each collected spectrum. In this experiment, the infrared spectrometer measures the downstream methanol concentration as a function of time, where permeability is determined from the slope of this early time data. Each experiment was conducted at 25 °C with a 2.0 M methanol feed concentration. The reported permeability value for each membrane is the average of multiple (at least three) experiments, where the standard deviation for each membrane was less than 15% of the average. This technique was developed in previous work.[10]

2.5. Small-Angle X-ray Scattering. Small-angle X-ray scattering experiments were performed at the multiangle X-ray scattering (MAXS) facility at the University of Pennsylvania. Specialty software (Datasqueeze Software developed by Paul A. Heiney at the University of Pennsylvania; www.datasqueezesoftware.com) was used to reduce two-dimensional data to one-dimensional intensity vs scattering vector (q) plots. The X-ray wavelength employed was 1.54 Å. The calibration standard was silver behenate, and the sample-to-detector distance was 55.0, 47.4, and 120 cm for the ion content, solvent casting, and annealing studies, respectively.

2.6. Sorption. Polymer samples weighing ∼50 mg were weighed before and after immersion (for a minimum of 1 week) in deionized water. Water sorption (uptake) is defined here as

$$\text{wt \%} = \left(\frac{\text{wet polymer wt} - \text{dry polymer wt}}{\text{dry polymer wt}}\right) \times 100 \qquad (2)$$

A balance with 0.01 mg accuracy was used. Three experiments were conducted on each sample, and the values reported are the average of these experiments. The standard deviations were less than 5% of these averaged values.

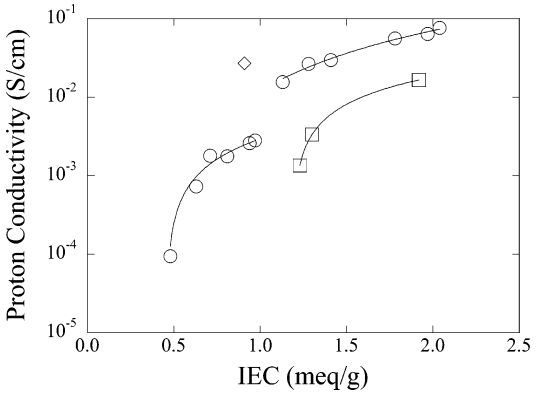

Figure 1. Proton conductivity vs IEC for Nafion 117 (◇), S-SIBS (○), and S-PS (□) membranes. The solid lines are trend lines.

3. Results and Discussion

3.1. Effect of Ion Content on Transport Properties. Figure 1 shows the proton conductivities as a function of IEC for Nafion 117, S-PS, and S-SIBS. Note that the conductivity of S-PS-0, S-PS-6, S-SIBS-0, and S-SIBS-13 could not be measured. At an IEC of ∼0.46 and 1.19 mequiv/g, the onset of the percolation threshold is observed for S-SIBS and S-PS, respectively. The percolation threshold is the critical ion content required for connectivity to occur between ionic domains providing transport pathways for ions and solvents to permeate across the membrane. Although the percolation threshold is much higher in S-PS compared to S-SIBS based on IEC, both polymers have similar percolation thresholds based on mol % of styrene sulfonated (∼13−17 mol %). Above the percolation threshold the conductivity of S-SIBS and S-PS increases with increasing ion content. More specifically, for S-SIBS conductivity increases from 9.4×10^{-5} to 0.076 S/cm over an IEC range of 0.47−2.04 mequiv/g, while S-PS increases from 1.4×10^{-3} to 0.017 S/cm over an IEC range of 1.23−1.92 mequiv/g. Carretta et al.[7] report similar conductivities for S-PS at similar ion contents and also report a similar percolation threshold (∼15 mol %).

Interestingly, there is a discontinuity in the trend in proton conductivity for S-SIBS membranes as a function of IEC. This is addressed in more detail in the subsequent sections in relation to polymer morphology and percolation theory.

In addition, the conductivity values for S-SIBS membranes are ∼1 order of magnitude greater than S-PS at similar ion contents. This result suggests that the difference in molecular architecture between the block copolymer (S-SIBS) and random copolymer (S-PS) leads to differences in morphology and therefore transport properties. Ding et al.[16] report similar findings in a comparison of a graft copolymer (PS-*g*-PSSA, where PSSA is poly(styrenesulfonic acid)) to a random copolymer (PS-*r*-PSSA or sulfonated polystyrene). The graft copolymer was an order of magnitude higher in proton conductivity compared to the random copolymer at similar ion contents. Their study suggests that differences in morphology as evidenced by transmission electron microscopy leads to these changes in transport properties.

The proton conductivity of Nafion 117 and S-SIBS-17, -22, -25, -34, and -36 membranes were measured in previous studies[10,19] and are compared to S-PS and S-SIBS-29, -42, -46, -54, -70, -79, and -82 in Figure 1. The conductivity of Nafion 117 is similar to values reported in the literature using a similar

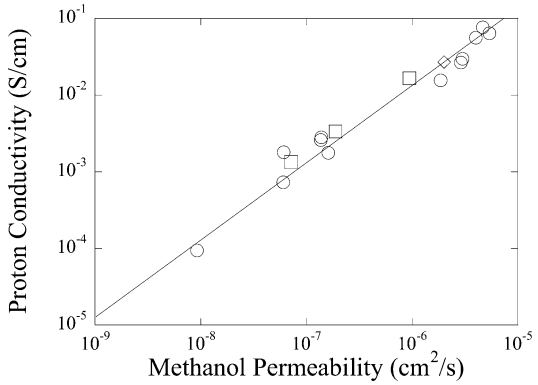

Figure 2. Proton conductivity vs methanol permeability for Nafion 117 (◇), S-SIBS (○), and S-PS (□) membranes. The solid line represents a linear regression of the data, where the slope is the selectivity (proton conductivity/methanol permeability = 1.32×10^4 S s/cm^3).

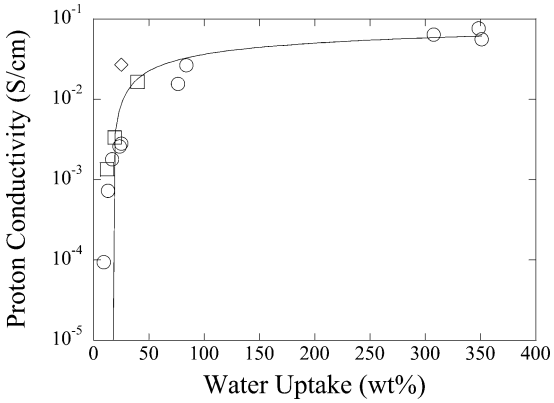

Figure 3. Proton conductivity vs water uptake for Nafion 117 (◇), S-SIBS (○), and S-PS (□) membranes. The solid line represents a trend line.

two-electrode technique: 0.024 S/cm,[34] 0.022 S/cm.[35] At a similar ion content, the proton conductivity of Nafion 117 (0.027 S/cm at 0.91 mequiv/g) is an order of magnitude greater than S-SIBS-34 (0.0026 S/cm at 0.94 mequiv/g); however, at double the IEC of Nafion 117, S-SIBS-82 (0.0764 S/cm at 2.04 mequiv/g) is approximately 3-fold higher in conductivity compared to Nafion 117. There are several possible reasons for lower conductivity of S-SIBS compared to Nafion 117 at similar ion contents, such as the differences in morphology and chemistry. Previous research[19] using SAXS has shown that S-SIBS membranes in the ion content range of 0.5−1.0 mequiv/g possess an anisotropic lamellar morphology with a preferred orientation in the plane of the membrane. Subsequently, there was a 10-fold difference in proton conductivity when measured parallel to the plane (four-electrode technique) compared to perpendicular to the plane (two-electrode technique) of the membrane. The difference in proton conductivity for Nafion 117 was only 2.5 times when comparing the two techniques. Gardner and Anantaraman[34] also reported similar differences in the conductivity of Nafion 117 when comparing these two measurement techniques and have suggested that these differences are primarily due to the differences between the two techniques and that Nafion 117 is isotropic. Another reason for differences in conductivity may be a result of the chemical differences between the fluoroether sulfonic acid side group in Nafion 117 compared to the phenylsulfonic acid side group in S-SIBS. Kreuer[36] reports a pK_a of −6 for Nafion compared to −1 for a sulfonated aromatic polymer, resulting in higher conductivities for Nafion.

Figure 2 shows proton conductivity vs methanol permeability for the membranes, and the line represents a linear regression to the data. The slope of the line corresponds to a selectivity (i.e., proton conductivity/methanol permeability) of 1.32×10^4 S s/cm^3. Surprisingly, these membranes appear to have similar selectivities (ranging from $\sim 1 \times 10^4$ to 3×10^4 S s/cm^3, where Nafion 117 has a selectivity of 1.35×10^4 S s/cm^3) regardless of chemistry or morphology. This suggests that protons and methanol have similar molecular transport mechanisms. Several membranes display slightly higher selectivities compared to that of Nafion 117, such as S-SIBS-25 (2.95×10^4 S s/cm^3) and S-SIBS-82 (1.63×10^4 S s/cm^3). However, although S-SIBS-25 has a methanol permeability that is 33 times lower than that of Nafion 117, the proton conductivity is 15 times lower. Similarly, although S-SIBS-82 has a proton conductivity ∼3 times higher than that of Nafion 117, the methanol permeability is ∼2 times higher. In summary, neither the S-SIBS-25 nor the S-SIBS-82 membranes are favorable alternatives because a membrane replacement for Nafion 117 for the direct methanol fuel cell should have a similar or higher proton conductivity with a lower methanol permeability. In other words, selectivity, which is just a ratio of proton conductivity to methanol permeability, should not be the only selection criteria.

Figure 3 shows proton conductivity as a function of water uptake, and unlike Figure 1, S-PS and S-SIBS have similar conductivities at similar water uptakes. For example, S-PS-15 (19.0 wt %, 0.0033 S/cm) is similar to S-SIBS-36 (24.9 wt %, 0.0028 S/cm), where Nafion 117 has a conductivity of 0.027 S/cm at 24.9 wt %. Methanol permeability follows a similar trend, where S-PS-15 (19.0 wt %, 1.89×10^{-7} cm^2/s) is similar to S-SIBS-36 (24.9 wt %, 1.39×10^{-7} cm^2/s), while Nafion 117 has a permeability of 2.01×10^{-6} cm^2/s at 24.9 wt %. Although Nafion 117 has a higher proton conductivity and methanol permeability at similar water uptake values, these data imply that water sorption is a primary factor in determining the selectivity in the polymers studied.

This can be understood by examining the proton conductivity and methanol permeability more thoroughly. The conductivity of protons can be derived from the Nernst−Planck equation:

$$\sigma_p = \frac{D_p C_p F^2}{RT} \tag{3}$$

where D_p, C_p, F, R, and T are the diffusion coefficient, concentration, Faraday's constant, gas constant, and temperature, respectively. The permeability of methanol can be defined as

$$P_m = D_m K_m \tag{4}$$

where D_m and K_m are the diffusion coefficient and partition coefficient (the ratio of methanol concentration inside the membrane to that in the adjacent solution), respectively. In eqs 3 and 4, D_p, D_m, and K_m are all functions of the water content or swelling in the polymer, which increases with increasing ion content, and C_p is also a function of ion content. In this study, the parameters that dictate both proton and methanol transport are similarly dependent on water concentration in the polymer. These two phenomena must be decoupled in order to increase selectivity. In other words, the proton diffusion coefficient must have a weaker dependence on water concentration or methanol must have a lower partition coefficient. Membranes with different proton conducting groups or selective chemical groups would be desired for increasing selectivity.

It is unclear why S-SIBS and S-PS have different relationships between ion content and water uptake. The morphological

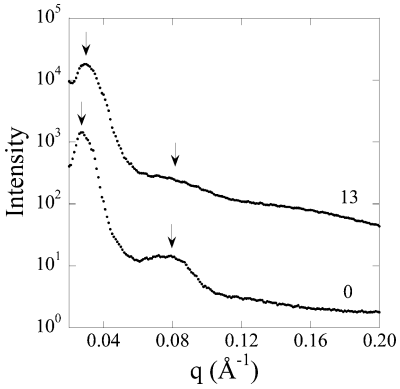

Figure 4. Small-angle X-ray scattering intensities as a function of scattering vector for S-SIBS-0 and S-SIBS-13. X-ray beam was in the plane of the membrane. The intensity profiles are offset here for legibility. Both polymers were solvent-cast from toluene.

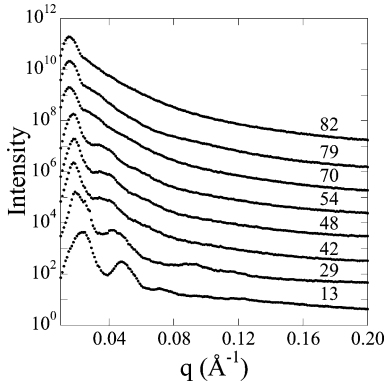

Figure 5. Small-angle X-ray scattering profiles for S-SIBS membranes ranging in IEC from 0.36 to 2.04 mequiv/g (S-SIBS-13, -29, -42, -48, -54, -70, -79, and -82). The X-ray beam was in the plane of the membrane. The intensity profiles are offset here for legibility. All polymers shown here were solvent-cast from a mixture of toluene/hexanol (85/15 w/w).

differences may lead to different uptakes at similar ion contents due to the variance in the amount of accessible ionic domains at different morphologies (e.g., isolated ionic domains). Also, it is interesting to note that although S-SIBS has a high water uptake at high IECs (348 wt % at 2 mequiv/g), it does not dissolve, where it has been documented that S-PS does dissolve at these IEC values.[37] The isobutylene midblock acts as a physical cross-linker to maintain an insoluble membrane with high proton conductivities at high IECs. Although membranes at these high water uptakes and methanol permeabilities may not be suitable for the DMFC, other ionic block copolymers with similar properties may be suitable for hydrogen fuel cells at low humidity conditions.

3.2. Effect of Ion Content on Polymer Structure. SAXS experiments were conducted on S-SIBS membranes to determine the polymer morphology at various ion contents and their effects on transport properties. Figure 4 shows the intensity profiles (I vs q) for S-SIBS-0 and S-SIBS-13, where both of these membranes were solvent-cast from pure toluene. The scattering vector, q, can be defined as

$$q = \frac{4\pi \sin(\theta)}{\lambda} \tag{5}$$

where 2θ and λ are the scattering angle and wavelength, respectively. Figure 4 shows distinct reflections in the intensity maxima located at the scattering vector positions: q_1 and $\sqrt{7}q_1$ for both S-SIBS-0 and S-SIBS-13, where q_1 is the first-order reflection. A scattering pattern with maxima in the vector positions q_1, $\sqrt{3}q_1$, $2q_1$, $\sqrt{7}q_1$, and $\sqrt{9}q_1$ is indicative of a hexagonally packed cylindrical morphology. It appears that S-SIBS-0 and S-SIBS-13 contain a cylindrical morphology; however, long-range order is not prevalent in these samples indicated by the broad scattering peaks and a lack of clearly defined scattering peaks at higher scattering vector positions. Crawford et al.[38] report a cylindrical morphology for S-SIBS-0, where long-range order increases with decreasing solvent evaporation rate. In this study the evaporation rate of the solvent was not controlled, but rather the membranes were solution cast in open Teflon Petri dishes.

Figure 5 shows the SAXS intensity profiles for S-SIBS membranes as a function of ion content (13−82 mol % sulfonation), where all of these membranes were solution-cast from a mixture of toluene/hexanol (85/15 w/w). Figure 5 shows a number of different profiles, where S-SIBS-13 and S-SIBS-29 display a periodic distribution with distinct reflections in the intensity maxima located at the scattering vector positions: q_1, $2q_1$, $3q_1$, $4q_1$, $5q_1$, and $6q_1$. This scattering pattern specifically corresponds to a lamellar morphology. These results corroborate with another study,[19] where SAXS data on similar S-SIBS membranes ranging in ion content from 0.5 to 1.0 mequiv/g (17−36 mol % sulfonation) reveal a lamellar morphology.

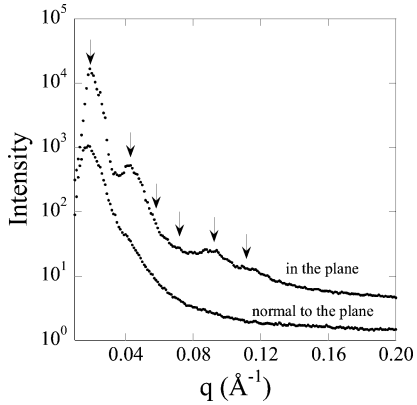

Figure 6. Small-angle X-ray scattering profiles for S-SIBS-29 (0.81 mequiv/g) for X-ray directions both in the plane and normal to the plane of the membrane.

Figure 6 shows the scattering profiles for two different X-ray orientations, in the plane and normal to the plane of the same membrane (S-SIBS-29). Scattering normal to the plane of the membrane shows weak scattering and no evidence of a periodic morphology in this orientation. These results reveal an anisotropic structure, where the lamellar domains are oriented in the plane of the membrane. These patterns were also observed in S-SIBS-13 and similarly in S-SIBS membranes ranging in ion content from 0.5 to 1.0 mequiv/g (17−36 mol % sulfonation) examined in another study.[19]

As ion content increases above 1.0 mequiv/g in S-SIBS membranes, it appears that the long-range order is disrupted (shown in Figure 5), which is indicated by the disappearance of clearly defined scattering peaks at higher scattering vector positions. This suggests a periodic-to-nonperiodic transition at higher ion contents or that increasing ion content in ionic block copolymers disrupts the block copolymer morphology. Interestingly, this change from a periodic lamellar to a nonperiodic morphology just above 1.0 mequiv/g corresponds to a discontinuity in the trend in the proton conductivity data shown in Figure 1.

Another parameter of interest is the Bragg spacing, which has been interpreted as an average domain spacing and can be calculated from Bragg's law:

$$d_1 = \frac{2\pi}{q_1} \tag{6}$$

The Bragg spacing, d_1, is determined from the maximum in the first-order reflection, q_1, in the SAXS intensity profile. The values for Bragg spacing calculated for all S-SIBS membranes are listed in Table 2. The Bragg spacing increases with increasing ion content (0−2.0 mequiv/g) from 23.3 to 41.9 nm. This may occur if increasing ion content results in larger ion clusters, which therefore impacts block copolymer morphology.

3.3. Effect of Ion Content on Structure−Transport Property Relationships. To understand the relationship between structure and transport properties (i.e., the discontinuity in transport data coinciding with the morphological transition), the transport data were analyzed with respect to a percolation model. For ion-containing polymers that follow a percolation model, no transport occurs below the percolation threshold, and transport above the threshold is a function of the excess volume fraction:

$$\frac{\sigma}{\sigma_0} \propto \frac{D}{D_0} \propto (\phi_1 - \phi_{1,c})^{\gamma_D} \tag{7}$$

where σ and D are the observed conductivity and diffusivity, respectively, and σ_0 and D_0 are the inherent conductivity and diffusivity in the diffusing phase, respectively. γ_D is the critical exponent for diffusion, ϕ_1 is the volume fraction of the diffusing or minority phase, $\phi_{1,c}$ is the critical volume fraction for percolation, and $(\phi_1 - \phi_{1,c})$ is the excess volume fraction. Values for γ_D give an indication of the randomness of the polymer structure. At high values (e.g., 1.6−1.7) the structure is nonideal or random, and at low values (e.g., 0.3−0.4) the structure is more ideal or aligned.[39]

Figure 7 shows a log−log plot of proton conductivity as a function of excess volume fraction in the polymer for S-SIBS membranes, where the lines correspond to a regression to the power law-based percolation model (eq 7). The data for the periodic lamellar morphology compared to the nonperiodic morphology regressed to two different slopes, where the critical exponents for diffusion, γ_D, are 1.22 and 0.67 for the lamellar (0.5−1.0 mequiv/g) and nonperiodic morphologies (1.1−2.0 mequiv/g), respectively. The critical volume fraction and critical exponent determined from this study are listed in Table 3, along with other percolation values determined from previous studies on ion conducting polymers.[11−15,19] The value of $\phi_{1,c}$ is 0.077, which matches another study on S-SIBS in this ion content range.[19] Note that the volume fraction (ϕ_i) was calculated from the water uptake and density of the polymer, which were both measured previously,[10,33] and the critical volume fraction, $\phi_{1,c}$, (i.e., percolation threshold) was determined from the *x*-axis intercept of the plot of conductivity vs volume fraction using data close to the percolation threshold (0.5−1.0 mequiv/g).

The critical exponent for diffusion for S-SIBS membranes at lower ion contents ($\gamma_D = 1.22$) is similar to other studies ($\gamma_D = 1.3-1.7$), indicating a more random structure (transport is in the opposite direction of the preferred orientation of the lamellar domains). At higher ion contents, the critical exponent for diffusion ($\gamma_D = 0.67$) is lower, indicating a more ideal structure. However, SAXS data reveal a lack of periodicity in the structure of these membranes at high ion contents. The percolation analysis suggests that a conversion from transport against the direction of oriented domains to transport in an isotropic structure (nonperiodic cocontinuous ionic network) provides less resistance in the membrane, therefore resulting in a more favorable structure for transport (illustrated in Figure 8).

Table 2. Bragg Spacing of S-SIBS Membranes as a Function of Ion Content

sample name	d_1 (nm)	sample name	d_1 (nm)
S-SIBS-0[a]	23.3	S-SIBS-36[b]	28.7
S-SIBS-13[a]	20.9	S-SIBS-42	34.9
S-SIBS-13	26.2	S-SIBS-48	33.1
S-SIBS-17[b]	26.3	S-SIBS-54	34.9
S-SIBS-22[b]	27.9	S-SIBS-70	41.9
S-SIBS-25[b]	29.7	S-SIBS-79	41.9
S-SIBS-29	33.1	S-SIBS-82	41.9
S-SIBS-34[b]	27.9		

[a] Solution cast from toluene. All other samples were solvent cast from a 85/15 (w/w) mixture of toluene/hexanol. [b] Reported previously.[19]

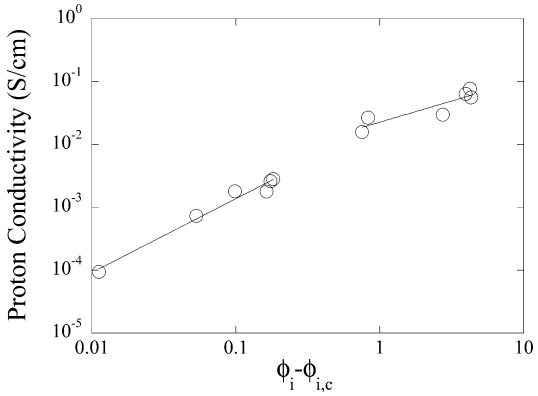

Figure 7. A log−log plot of proton conductivity vs excess volume fraction of the diffusing phase in S-SIBS membranes. The solid lines represent a regression to the percolation model.

3.4. Effect of Casting Solvent on Structure−Transport Properties. Tables 4 and 5 lists the measured proton conductivities of S-SIBS-29 membranes solution cast from 15 different solvents at a constant ion content (0.81 mequiv/g). Although all membranes have the same IEC, the proton conductivities vary by almost 3 orders of magnitude, ranging from 1.07×10^{-5} S/cm (toluene/ethanol (85/15 w/w)) to 5.95×10^{-3} S/cm (toluene). Kim et al.[40] report only 1 order of magnitude increase in both proton conductivity and methanol permeability for a sulfonated poly(styrene-*b*-ethylene-*r*-butylene-*b*-styrene) block copolymer cast from two different solvents, THF and a mixture of THF/methanol, at the same ion content (27 mol %). Their study also reports a morphological change from lamellar to a nonperiodic structure with the introduction of methanol in the solvent, where the nonperiodic morphology enhances transport. Kim et al.[40] also examined SAXS of both dry and hydrated sulfonated block copolymers and report similar morphologies with a slight increase in Bragg spacing when the polymers are hydrated. All SAXS experiments conducted on S-SIBS membranes in this study were examined in the dry state.

The morphology was also investigated in this study as a function of casting solvent. Figure 9 shows the SAXS intensity profiles for S-SIBS-29 solution cast from five different solvents: chloroform (-CF), methylene chloride (-MC), cyclohexanol (-CH), benzene (-BZ), and tetrahydrofuran (-THF). Membranes increasing in proton conductivity are arranged from bottom to top in Figure 9, and all of the SAXS data correspond to scattering in the plane of the membrane. There are distinct differences in the scattering profiles between these samples. S-SIBS-29 membranes show distinct reflections in the intensity maxima located at the scattering vector positions: q_1, $\sqrt{3}q_1$, $\sqrt{7}q_1$ (chloroform); q_1, $2q_1$, $\sqrt{7}q_1$ (methylene chloride); q_1, $2q_1$, $3q_1$ (cyclohexane); q_1, $2q_1$, $\sqrt{7}q_1$ (benzene); q_1, $2q_1$, $3q_1$, $4q_1$,

Table 3. Percolation Values

polymer name	γ_D[a]	$\phi_{1,c}$[b]	ref
Nafion	1.5 ± 0.02	0.10	11
poly(methyl methacrylate-*co*-methacrylic acid)	1.35	0.26	12
poly(styrene-*co*-methacrylic acid)	1.7	0.17	13
sulfonated poly(phenylene oxide)	1.5	0.16	14
sulfonated poly[bis(3-methylphenoxy)phosphazene]	1.26	0.18−0.25	15
S-SIBS (0.5−1.0 mequiv/g)	1.22	0.077	19
S-SIBS (1.1−2.0 mequiv/g)	0.67	0.077	this work

[a] Critical exponent for diffusion. [b] Critical volume fraction.

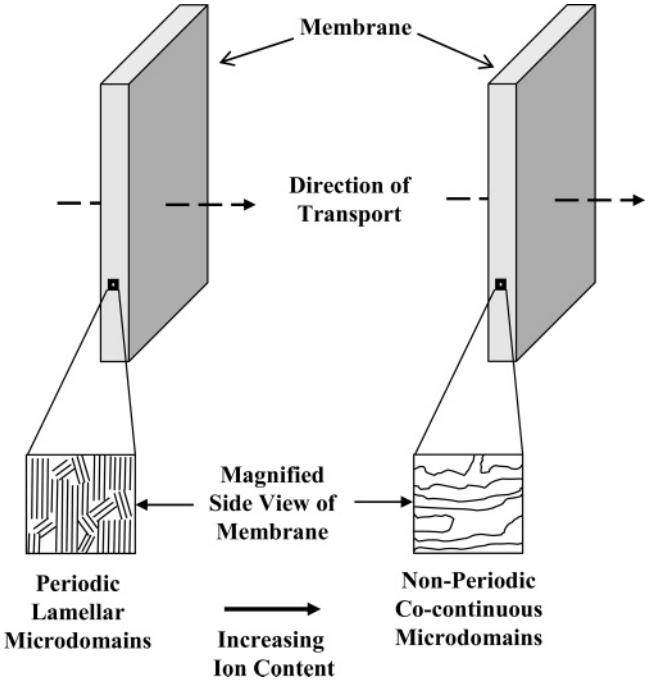

Figure 8. Illustration depicting the morphological change with increasing ion content. At low ion contents, a periodic lamellar morphology exists, where the microdomains are predominantly oriented perpendicular to the direction of transport. At higher ion contents, a nonperiodic cocontinuous morphology exists providing less resistance for transport.

Table 4. Proton Conductivity of S-SIBS-29 Membranes as a Function of Casting Solvent at a Constant Ion Content (0.81 mequiv/g)

casting solvent	proton conductivity (S/cm) (×10²)
toluene	0.595
toluene/ethanol (85/15 w/w)	0.00107
toluene/2-propanol (85/15 w/w)	0.265
toluene/butanol (85/15 w/w)	0.198
toluene/hexanol (99/1 w/w)	0.198
toluene/hexanol (95/5 w/w)	0.159
toluene/hexanol (90/10 w/w)	0.248
toluene/hexanol (85/15 w/w)	0.204
toluene/hexanol (80/20 w/w)	0.225

$5q_1$ (THF). Aside from S-SIBS-29-THF (lamellar), a high level of long-range order is not apparent in S-SIBS-29 membranes cast from other solvents, which is indicated by broad scattering peaks and a lack of clearly defined scattering peaks at larger scattering vectors.

From these scattering patterns it is difficult to draw definitive conclusions regarding structure−transport property relationships. Unlike the effect of changing ion content, casting S-SIBS at a constant ion content from different solvents results in similar water uptakes.[41] Therefore, it is clear that different solvents induce different morphologies, which therefore significantly impact transport properties. Additionally, methanol permeability

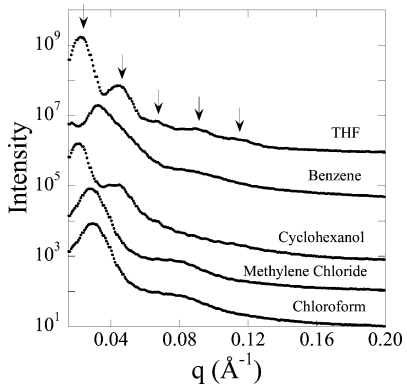

Figure 9. Small-angle X-ray scattering intensities as a function of scattering vector for S-SIBS-29 (0.81 mequiv/g) cast form different solvents (X-ray beam was in the plane of the membrane). The intensity profiles are offset here for legibility.

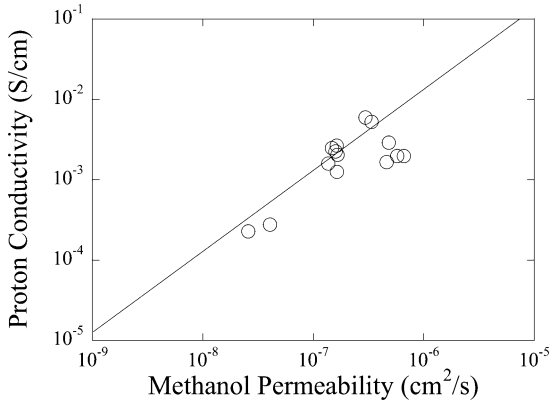

Figure 10. Proton conductivity vs methanol permeability for S-SIBS-29 (0.81 mequiv/g) as a function of different casting solvents. The solid line represents a linear regression of the data in Figure 2, where the slope corresponds to selectivity (proton conductivity/methanol permeability).

Table 5. Proton Conductivity and Bragg Spacing of S-SIBS-29 Membranes as a Function of Casting Solvent at a Constant Ion Content (0.81 mequiv/g)

casting solvent	proton conductivity (S/cm) (×10²)	d_1 (nm)
chloroform	0.0229	20.4
cyclohexanone	0.0277	
methylene chloride	0.125	25.4
cyclohexanol	0.166	28.4
benzene	0.291	18.8
tetrahydrofuran	0.522	26.3

follows a similar trend compared to proton conductivity, shown in Figure 10, where the selectivities of most of the polymers are similar regardless of casting solvent. The values for Bragg spacing calculated for S-SIBS membranes as a function of casting solvent are listed in Table 5. Bragg spacing varies from 18.8 to 28.4 nm with no apparent coinciding trend with transport properties.

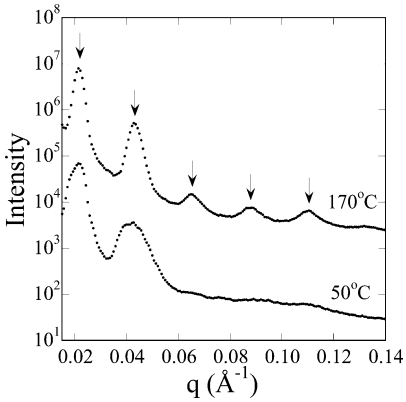

Figure 11. Small-angle X-ray scattering profiles for S-SIBS-22 (0.63 mequiv/g) annealed at 50 and 170 °C. The X-ray beam was in the plane of the membrane. The intensity profiles are offset here for legibility. The polymer membrane was solvent cast from THF.

Block copolymer morphology changes upon differences in annealing,[42] shear forces,[43] solvent choice,[44] solvent evaporation rate,[45] and film thickness[46] have been well documented. Although the change in the morphology of block copolymers by varying choice of casting solvent has been considered by a number of investigators, this has not been well studied in ionic block copolymers.[40] In block copolymers, interaction between the solvent and each block and the solvent vapor pressure can play a role in the resulting morphology. After reviewing various solvent properties (boiling point, solubility parameter, and dielectric constant), there appears to be no obvious correlation between any of these properties and proton conductivities listed in Tables 4 and 5. However, there may be a synergetic effect from a number of parameters during solvent casting. The significant differences in transport properties merit further investigation on the effect of solvent choice on ionic block copolymer structure.

3.5. Effect of Annealing on Polymer Structure. SAXS intensity profiles for S-SIBS-0 (toluene), S-SIBS-22 (toluene), and S-SIBS-22 (THF) annealed at both 50 and 170 °C were investigated. The scattering pattern for S-SIBS-0 annealed at 50 °C is similar to Figure 4, where there is no apparent long-range order. However, S-SIBS-0 annealed at 170 °C reveals a high level of long-range order with a scattering pattern with maxima in the vector positions q_1, $\sqrt{3}q_1$, $2q_1$, $\sqrt{7}q_1$, and $\sqrt{9}q_1$, which is indicative of a hexagonally packed cylindrical morphology. However, there was no long-range order for S-SIBS-22 (0.63 mequiv/g) solution cast from toluene at either annealing temperature. Although, there is a shift in the maximum in the first-order reflection, q_1, in the SAXS intensity profile between the sample annealed at 50 and 170 °C, which corresponds to a change in Bragg spacing from ~20 to 25 nm. SAXS intensity patterns for S-SIBS-22 solution cast from THF show a transition from a low to a high level of long-range order from the sample annealed at 50−170 °C, respectively (Figure 11). S-SIBS-22 annealed at 170 °C revealed a lamellar morphology with intensity maxima located at the scattering vector positions q_1, $2q_1$, $3q_1$, $4q_1$, and $5q_1$.

X-ray scattering profiles for S-SIBS-22 solution cast from THF and annealed at 170 °C also reveal an anisotropic structure, where the lamellar domains are preferentially oriented in the plane of the membrane. This was not observed in the sample that was annealed at 50 °C. Furthermore, S-SIBS-0 solution cast from toluene showed slight orientation in the plane of the membrane when annealed at 170 °C compared to no orientation when annealed at 50 °C. S-SIBS-22 solution cast from toluene showed no orientation at either annealing temperature. These results demonstrate that annealing above the glass transition temperature of polystyrene can increase long-range order in S-SIBS, but this is dependent on the solvent choice.

4. Conclusions

In this study, structure−transport property relationships of an ionic block copolymer were investigated as a function of ion content (particularly at high ion contents) and casting solvent. The block copolymer architecture provides a framework that increases transport properties by an order of magnitude when compared to random copolymers of similar chemistry and ion content. Furthermore, increasing ion content in the ionic block copolymer induces a periodic-to-nonperiodic transition in polymer structure. High ion contents disrupt the block copolymer morphology, resulting in a cocontinuous ionic network, which abruptly increases transport. Percolation analysis suggests that this conversion from transport against the direction of anisotropic oriented domains to transport in a cocontinuous isotropic structure provides less resistance in the membrane, therefore resulting in a more favorable structure for transport. In addition, morphological differences occur with casting solvent choice resulting in transport differences of almost 3 orders of magnitude. These results illustrate the impact of chain architecture and processing conditions on the polymer morphology and subsequently on the transport in ionic block copolymers.

In addition, the ionic block copolymer in this study possessed a 3-fold higher conductivity compared to that of Nafion 117 at an IEC of 2.0 mequiv/g. However, this polymer contained a much higher water uptake (348 wt %) compared to that of Nafion 117 (~25 wt %). Interestingly, the ionic block copolymer did not dissolve in water at these high ion contents, where it has been documented that sulfonated polystyrene does dissolve at these ion contents. Here, the rubber midblock acts as a physical cross-linker to maintain an insoluble membrane with high proton conductivities at high ion contents. Although, membranes at these high water uptakes and methanol permeabilities may not be suitable for the DMFC, ionic block copolymers similar to these may be suitable for hydrogen fuel cells at low humidity conditions.

All of the polymers examined in this study possessed similar selectivities regardless of chemistry or morphology. This suggests that protons and methanol have similar molecular transport mechanisms in sulfonic acid-containing polymers, and water sorption may be a dominant factor for selectivity. Polymers with different proton conducting groups or selective chemical groups are desired for increasing selectivity for application to the DMFC.

Acknowledgment. A portion of this research was conducted while Y. A. Elabd held a National Research Council Research Associateship Award at the U.S. Army Research Laboratory. Y. A. Elabd acknowledges the financial support of the U.S. Army Research Office through agreement W911NF-04-1-0258. K. I. Winey acknowledges the financial support of the U.S. Army Research Office through agreement DAAD-190310130.

References and Notes

(1) U.S. Department of Energy. *Fuel Cell Handbook*, 6th ed.; B/T Books: Orinda, CA, 2002.
(2) Scott, K.; Taama, W. M.; Argyropoulos, P.; Sundmacher, K. *J. Power Sources* **1999**, *83*, 204.
(3) Brandon, N. P.; Skinner, S.; Steele, B. C. H. *Annu. Rev. Mater. Res.* **2003**, *33*, 183.
(4) Eisenberg, A.; King, M. *Ion Containing Polymers: Physical Properties and Structure*; Academic Press: New York, 1977.

(5) Hsu, W. Y.; Barkley, J. R.; Meakin, P. *Macromolecules* **1980**, *13*, 198.
(6) Mauritz, K. A.; Moore, B. *Chem. Rev.* **2004**, *104*, 4535.
(7) Carretta, N.; Tricoli, V.; Picchioni, F. *J. Membr. Sci.* **2000**, *166*, 189.
(8) Yeo, R. S.; Yeager, H. L. In *Perfluorinated Ionomer Membranes*; Eisenberg, A., Yeager, H. L., Eds.; American Chemical Society: Washington, DC, 1980; pp 437−505.
(9) Zawodzinski, T. A.; Derouin, C.; Radzinski, S.; Sherman, R. J.; Smith, V. T.; Springer, T. E.; Gottesfeld, S. *J. Electrochem. Soc.* **1993**, *140*, 1041.
(10) Elabd, Y. A.; Napadensky, E.; Sloan, J. M.; Crawford, D. M.; Walker, C. W. *J. Membr. Sci.* **2003**, *217*, 227.
(11) Hsu, W. Y.; Barkley, J. R.; Meakin, P. *Macromolecules* **1980**, *13*, 198.
(12) Gronowski, A. A.; Jiang, M.; Yeager, H. L.; Wu, G.; Eisenberg, A. *J. Membr. Sci.* **1993**, *82*, 83.
(13) Matsuyama, H.; Teramoto, M.; Tsuchiya, M. *J. Membr. Sci.* **1996**, *118*, 177.
(14) Tongwen, X.; Weihua, Y.; Bingling, H. *Chem. Eng. Sci.* **2001**, *56*, 5343.
(15) Tang, H.; Pintauro, P. N. *J. Appl. Polym. Sci.* **2001**, *79*, 49.
(16) Ding, J.; Chuy, C.; Holdcroft, S. *Chem. Mater.* **2001**, *13*, 2231.
(17) Cable, K. M.; Mauritz, K. A.; Moore, R. B. *Chem. Mater.* **1995**, *7*, 1601.
(18) Maki-Ontto, R.; de Moel, K.; Polushkin, E.; van Ekenstein, G. A.; ten Brinke, G.; Ikkala, O. *Adv. Mater.* **2002**, *14*, 357.
(19) Elabd, Y. A.; Beyer, F. L.; Walker, C. W. *J. Membr. Sci.* **2004**, *231*, 181.
(20) Hamley, I. W. *The Physics of Block Copolymers*; Oxford University Press: New York, 1998.
(21) Weiss, R. A.; Sen, A.; Pottick, L. A.; Willis, C. L. *Polymer* **1991**, *32*, 2785.
(22) Gouin, J. P.; Williams, C. E.; Eisenberg, A. *Macromolecules* **1989**, *22*, 4573.
(23) Weiss, R. A.; Sen, A.; Willis, C. L.; Pottick, L. A. *Polymer* **1991**, *32*, 1867.
(24) Lu, X.; Steckle, W. P.; Weiss, R. A. *Macromolecules* **1993**, *26*, 5876.
(25) Venkateshwaran, L. N.; York, G. A.; DePorter, C. D.; McGrath, J. E.; Wilkes, G. L. *Polymer* **1992**, *33*, 2277.
(26) Storey, R. F.; Chisholm, B. J.; Lee, Y. *Polym. Eng. Sci.* **1997**, *37*, 73.
(27) Kim, J.; Kim, B.; Jung, B. *J. Membr. Sci.* **2002**, *207*, 129.
(28) Edmondson, C. A.; Fontanella, J. J.; Chung, S. H.; Greenbaum, S. G.; Wnek, G. E. *Electrochim. Acta* **2001**, *46*, 1623.
(29) Mokrini, A.; Del Rio, C.; Acosta, J. L. *Solid State Ionics* **2004**, *166*, 375.
(30) Shin, C. K.; Maier, G.; Andreaus, B.; Scherer, G. G. *J. Membr. Sci.* **2004**, *245*, 147.
(31) Yang, Y.; Shi, Z.; Holdcroft, S. *Macromolecules* **2004**, *37*, 1678.
(32) Yang, Y.; Lee, J. *Electrochim. Acta* **2004**, *50*, 617.
(33) Elabd, Y. A.; Napadensky, E. *Polymer* **2004**, *45*, 3037.
(34) Gardner, C. L.; Anantaraman, A. V. *J. Electroanal. Chem.* **1995**, *395*, 67.
(35) Pourcelly, G.; Oikonomou, A.; Gavach, C.; Hurwitz, H. D. *J. Electroanal. Chem.* **1990**, *287*, 43.
(36) Kreuer, K. D. *J. Membr. Sci.* **2001**, *185*, 29.
(37) Baigl, D.; Seery, T. A. P.; Williams, C. E. *Macromolecules* **2002**, *35*, 2318.
(38) Crawford, D. M.; Napadensky, E.; Tan, N. C. B.; Reuschle, D. A.; Mountz, D. A.; Mauritz, K. A.; Laverdure, K. S.; Gido, S. P.; Liu, W.; Hsiao, B. *Thermochim. Acta* **2001**, *367−368*, 125.
(39) Kirkpatrick, S. *Rev. Mod. Phys.* **1973**, *45*, 574.
(40) Kim, J.; Kim, B.; Jung, B.; Kang, Y. S.; Ha, H. Y.; Oh, I.-H.; Ihn, K. J. *Macromol. Rapid Commun.* **2002**, *23*, 753.
(41) Suleimann, D.; Elabd, Y. A.; Napadensky, E.; Sloan, J. M.; Crawford, D. M. *Thermochim. Acta* **2005**, *430*, 149.
(42) Hajduk, D. A.; Gruner, S. M.; Rangarajan, P.; Register, R. A.; Fetters, L. J.; Honeker, C.; Albalak, R. J.; Thomas, E. L. *Macromolecules* **1994**, *27*, 490.
(43) Morrison, F. A.; Winter, H. H. *Macromolecules* **1989**, *22*, 3533.
(44) Funaki, Y.; Kumano, K.; Nakao, T.; Jinnai, H.; Yoshida, H.; Kimishima, K.; Tsutsumi, K.; Hirokawq, Y.; Hashimoto, T. *Polymer* **1999**, *40*, 7147.
(45) Libera, M.; Kim, G. *Macromolecules* **1998**, *31*, 2569.
(46) Heck, B.; Arends, P.; Ganter, M.; Kressler, J.; Stuhn, B. *Macromolecules* **1997**, *30*, 4559.

MA051958N